Position-dependent attenuation by Kv1.6 of N-type inactivation of Kv1.4-containing channels

Macdara Bodeker, Ahmed Al-Sabi, Marie Le Berre, J. Oliver Dolly

2/19/2011

Position-dependent attenuation by Kv1.6 of N-type inactivation of Kv1.4-containing channels

MacDara Bodeker[1], Ahmed Al-Sabi[1], Marie Le Berre, and J. Oliver Dolly[2]

International Centre for Neurotherapeutics, Dublin City University, Glasnevin, Dublin 9, Ireland.

Short title: NIP interactions in Kv1 hetero-tetramers

[1] The first two authors contributed equally to this work.
[2]To whom correspondence should be addressed (Fax: +35317007758, E-mail: oliver.dolly@dcu.ie).

Assembly of distinct α subunits of voltage-gated K^+ channels (Kv1) into tetramers underlies the diversity of their outward currents in neurons. Kv1.4-containing channels normally exhibit N-type rapid inactivation, mediated through an N-terminal inactivation ball (NIB); this can be over-ridden if associated with a Kv1.6 α subunit, via its N-type inactivation prevention (NIP) domain. Herein, NIP function was shown to require positioning of Kv1.6 adjacent to the Kv1.4 subunit. Using a recently-devised gene concatenation, hetero-tetrameric Kv1 channels were expressed as single-chain proteins on the plasmalemma of HEK-293 cells, so their constituents could be arranged in different positions. Placing Kv1.4 and 1.6 genes together, followed by two copies of Kv1.2 yielded a K^+ current devoid of fast inactivation. Mutation of critical glutamates within the NIP endowed rapid inactivation. Moreover, separating Kv1.4 and 1.6 with a copy of Kv1.2 gave a fast-inactivating K^+ current with steady-state inactivation shifted to more negative potentials and exhibiting slower recovery. Alternatively, separating Kv1.4 and 1.6 with two copies of Kv1.2 yielded slowly-inactivating currents because in this concatamer Kv1.4 and 1.6 are together. These findings, also, confirm that the gene concatenation can generate K^+ channels with α subunits in pre-determined positions.

Keywords: Voltage-dependent gating, N-terminal domain, Kv1 hetero-tetramers, NIP, inactivation, Kv1.4-containing channels

The abbreviations: ATP, Adenosine 5′-triphosphate; bp, base pair; EGTA, Ethylene glycol-bis(2-aminoethylether)-N,N,N′,N′-tetra acetic acid; HEK, human kidney embryo; HEPES, 4-(2-Hydroxyethyl)-1-piperazine-ethanesulfonic acid; I_K, potassium current; Kv1, voltage-gated K^+ channels; NIB, N-terminal inactivation ball; NIP, N-type inactivation prevention domain; ORF, open reading frame; TBS, Tris-buffered saline; UTR, the untranslated region.

INTRODUCTION

Neuronal voltage-gated (Kv1) channels largely arise from hetero-tetramerisation of α subunits encoded by 7 major genes (Kv1.1-1.6 and Kv1.8) with 4 auxiliary Kvβ subunits [1,2,3]. As each α subunit contributes distinct properties, the resultant channels reaching the plasmalemma vary considerably in their pharmacological and biophysical properties. After opening of these Kv1 channels by membrane depolarisation, inactivation follows via two mechanisms. N-type inactivation mediated through the inactivation ball (NIB) occurs by a "ball and chain" process in which NIB occludes the inner mouth of the ion pore [4,5]. In addition, $Kv\beta_1$ subunits provide alternative N-terminal domains that confer rapid inactivation on non- or slowly-inactivating Kv1 channels [6-8]. On the other hand, C-type inactivation arises from prolonged depolarisation which leads to a local re-arrangement and constriction of the channel at the outer mouth [9-12]. Kv1.4 is the only Kv1 member that shows N- and C-type inactivation, yielding a distinctive A-type transient outward current [13].

Heteromerised Kv1.4 and 1.2 subunits have been localized in axons and nerve terminals, which may form the molecular basis of a pre-synaptic A-type K^+ channel involved in the regulation of neurotransmitter release [14]. Moreover, direct biochemical studies have revealed that Kv1.4 forms channel oligomers with Kv1.2 and 1.6 subunits in brain [15]. The fast N-type inactivation endowed by Kv1.4 can be prevented by the presence of Kv1.6 through its NIP (N-type inactivation prevention) domain [16], giving rise to a much slower inactivating/sustained K^+ current. As tetramerisation of Kv channel subunits occurs in the endoplasmic reticulum [17], pinpointing their ordering *in vivo* has, thus far, eluded researchers because of an inability to pre-determine the arrangement of their assembled constituents in the oligomers delivered to the cell surface. Therefore, it is warranted to focus efforts on gaining a clearer understanding of the influences of subunit ordering, particularly, as the resultant data could give insights into the modulation of neuronal transmission by Kv1 channels. Furthermore, such information is medically relevant given that delayed rectifier Kv1 subunits, but not Kv1.4, are down-regulated in the hippocampus of animal models prone to seizures [18], whereas Kv1.4 is up-regulated following chronic injury of the spinal cord [19].

Herein, a recently-designed expression platform [20] was utilised to express 4 Kv1 α constituents as a single open reading frame (ORF) in transfected HEK-293 cells, allowing pre-determination of not just the combinations of α subunits but, also, their actual arrangements in channels on the plasmalemma. This permitted a fundamental question to be answered, namely, whether subunit ordering influences the pharmacological and biophysical profiles of Kv1 channels. For this, advantage was taken of the NIP in Kv1.6 [16] being able to prevent fast inactivation of Kv1.4-containing channels. If NIP competes directly for the binding site of NIB, displacing it, giving rise to slow inactivation, no differences ought to be expected when these two α subunits are placed adjacently or distally in concatenated heteromers, with both of their currents inactivating slowly. On the other hand, if NIP function relies on it directly interacting with NIB, dissimilarities in inactivation rates may occur with a slowly-inactivating current only occurring when both domains are optimally placed. Suboptimal placement might result in a fast-inactivating channel where NIP is positioned away from NIB and unable to modulate it. To address this important question, for the first time, inactivation,

voltage-dependence of inactivation and recovery from inactivation were measured in three recombinantly-expressed tetramers, with identical subunit composition but distinct subunit ordering. The novel outcome of this approach questions the wisdom of predicting channel properties based on subunit content alone because their positioning greatly influences the channels' characteristics. Also, the data reaffirms, convincingly, that this concatenation of genes pre-determines the positions of α subunits in the assembled functional channels on the cell surface.

MATERIALS AND METHODS

PCR amplification and assembly of Kv1.X constituents

Concatenation of 4 α subunits as a single ORF (Figure 1A) was accomplished using an inter-subunit linker derived from the untranslated regions (UTR) of the *Xenopus* β globin gene (J00978) [21]. The cDNAs for rat Kv 1.2, 1.4 and 1.6 were kindly provided by Prof. Olaf Pongs (University of Hamburg, Germany). Amplification was carried out using Kv-sequence specific primers which incorporated flanking Xba I - Xho I sites (Supplementary Table 1, upper panel), allowing their individual cloning into a UTR-containing intermediate plasmid pβUT, at Xba I – Xho I cloning sites located between the 50 bp 5` UTR (FB750344) and the 150 bp 3` UTR (FB750345). A second round of PCR, using primers specific to the UTRs themselves, allowed amplification of the α subunit ORF contiguous with flanking UTRs. Paired restriction sites were also added (Supplementary Table 1 lower panel), facilitating position-specific direct cloning into pIRES2-DsRed. Kv1.2, 1.4 and 1.6 were individually subcloned into positions I to IV using paired sites for Nhe I/Bgl II, Bgl II/EcoR I, EcoRI/Sal I, and Sal I/BamH I, respectively (Figure 1A), each now separated by a combined 200 bp linker. After conventional restriction digestion and ligation, the final constructs were transformed into *E. coli* strain DH5α, screened by PCR and verified by complete sequencing. Correct positioning of the genes in all pIRES2-DsRed plasmid constructs was confirmed by restriction analysis (Supplemental Material Figure S1).

In vitro mutagenesis

NIP function of Kv1.6 was abolished by carrying out amino acid substitutions identified by others [16]. Briefly, Kv1.6 was amplified using *Pfx* polymerase (Invitrogen) in the presence of primers to mutate NIP residues Glu^{27}, Glu^{30} and Glu^{32} to alanines, thereby, yielding the mutant (Kv1.6 E27/30/32A) that was confirmed by DNA sequencing.

Gene expression and verification of hetero-tetrameric constructs

The Kv1 channel constructs were expressed in HEK-293 cells (American Type Culture Collection) for 24-48 h after transfection with Polyfect reagent (Qiagen, Crawley, UK). Cells were harvested, washed, resuspended at ~ 2-3x10^7 cells/ml in phosphate-buffered saline pH 7.4 (PBS) and incubated with sulfo-NHS-LC-biotin (1 mg/ml; Pierce, Rockford, IL) at room temperature for 30 min. Remaining reagent was quenched with 100 mM glycine for 30 min; samples were then solubilised in 2% Triton X-100 for 1 h at 4°C, and centrifuged at 100 000g for 1 h. The supernatant was incubated with streptavidin-agarose (70 µl slurry/ml; Pierce, Rockford, IL) overnight at 4°C with rotation. After washing the pelleted streptavidin-agarose with ice-cold Tris-buffered

saline, pH 7.9 (50 mM Tris-HCl, 150 mM NaCl) (TBS) containing 0.1% Tween-20, bound proteins were dissolved in SDS-PAGE sample buffer and monitored by SDS-PAGE followed by Western blotting with monoclonal Kv1 α subunit-specific antibodies (NeuroMab, Davis, CA, USA) The tetramers were visualized using a mouse secondary antibodies (Sigma-Aldrich, Ireland) conjugated to alkaline phosphatase with the substrate (5-bromo-4-chloro-3'-indolyphosphate p-toluidine Salt and nitro-blue tetrazolium chloride [Sigma-Aldrich, Ireland]). For fluorescence microscopy, HEK-293 cells were plated on poly-L-lysine-coated glass coverslips in 35mm dishes and transfected using Polyfect as described above, with the constructs encoding representative hetero-tetramers (Kv1.4-1.2-1.6-1.2, Kv1.4-1.6-1.2-1.2, and Kv1.4-1.2-1.2-1.6). The samples were processed for staining 48 h post-transfection as previously described [22]. Following fixation with 4% paraformaldehyde (PFA) in PBS, the cells were washed, blocked in TBS pH 7.4 /4% (w/v) dried milk for 60 min and permeabilised for 30 min with 0.1% Triton-X-100 in the blocking buffer. Cells were incubated with mouse anti-Kv1.2 or Kv1.4 IgGs for 1 h at room temperature. Washing was repeated prior to further incubation with goat anti-mouse IgG conjugated to Alexa Fluor 488 (Invitrogen, Dublin, Ireland) for 1h. The samples were thoroughly washed in PBS prior to being fixed with Vectashield (Vector Laboratories, UK). Control specimens were treated likewise except for omitting the first antibody. Confocal images were obtained with Observer Z1 Axion inverted microscope (LSM-710, Carl Zeiss). A 40 x 0.95 NA oil immersion objective was used for imaging with the pinhole diameter set for 1 Airy Unit. Fluor was excited with the 488 nm line of an Argon laser and emission bandpass was set at 492-636 nm.

Electrophysiological recordings and data analysis

Tetrameric Kv1 channel constructs were expressed in HEK-293 cells for 24-48 h after transfection as described above and split using a detaching agent, Accutase (Analab, Austria), onto glass coverslips before recording. All measurements were made using the whole-cell configuration of the voltage-clamp technique at -90 mV holding potential, as outlined before [21], except where specified. The recording pipettes were filled with an intracellular solution (in mM): 95 KF, 20 KCl, 1 $CaCl_2$, 1 $MgCl_2$, 11 EGTA, 10 HEPES, Na_2ATP (pH 7.2 with KOH), 10 glucose and 20 sucrose (300±10 mOsm), with tip resistances between 1.5-3.0 MΩ. To ensure functionality of the NIB moiety, 2 mM glutathione (Sigma-Aldrich, Ireland) was introduced as a reducing agent to the internal solution [16, 23]. External (bath) medium contained (in mM): 135 NaCl, 5 KCl, 2 $CaCl_2$, 2 $MgCl_2$ and 5 HEPES (pH 7.4 with NaOH). The liquid junction potential was not corrected. Only cells with series resistances <10 MΩ throughout the experiments were included in this study. Series resistance was compensated (75–80%) to minimize voltage errors. Currents were recorded with an EPC10 (HEKA Elektronik, Germany) patch-clamp amplifier. Leakage and capacitive currents were subtracted on-line using the P/4 subtraction protocol. Currents were filtered at 1 kHz, and sampled at 5 kHz (with the exception of 10 s pulses, which were sampled at 50 Hz). Time-dependent inactivation constants were determined during 10-sec depolarisation steps from -20 to 10 mV in 10 mV increments, and the currents fitted with double exponential functions [21]. For experiments on the recovery from inactivation, a variable interval-gapped pulse protocol was used: from -90 mV holding potential, depolarisation to +10 mV for 300 ms in an initial step followed by a second identical pulse with gap intervals of 0-20 s. The

ratios of the normalised peak currents at time intervals were plotted and fitted with a single exponential function to obtain time courses of recovery from inactivation. Measurement of steady-state inactivation involved a 10-sec conditioning pulse applied in 10 mV increments from -100 to +10 mV, followed by a 500 ms test pulse at +10 mV (at -90 mV holding potential). Steady-state inactivation constants were calculated from the peak currents of the test pulses. Normalized inactivation curves were fitted to the Boltzmann function ($I = [1 + \exp\{(V - V_{1/2}) / k\}]^{-1}$), where V is the membrane (pre-pulse) potential, $V_{1/2}$ is the potential at half-maximal inactivation, and k is the slope factor. Data (means ± S.E.M.; n is number of cells tested) were analysed using Pulsefit (HEKA Electronik, Germany) and fitted by Igor Pro 6 (WaveMetrics, OR, USA). Statistical significance was evaluated by Mann-Whitney U test, as appropriate, for data from at least three independent experiments; P values of < 0.05 were considered significant.

RESULTS

Channel concatemers of defined α subunit composition expressed following domain-specific assembly of gene cassettes into pIRES2-DsRed plasmid

Through examining the properties of recombinantly-expressed hetero-tetramers, a new strategy [20] has been validated for concatenating and expressing functional Kv1.X genes within a single ORF, on the plasmalemma of mammalian cells. Herein, two subunits, which play physiologically-important but opposing roles in determining Kv1 channel inactivation, were selected to obtain proof of principle for retaining their ordering according to positions within the gene constructs (Figure 1A). Kv1.4, which can mediate N-type inactivation of mammalian Kv1 channels through its NIB [23,24], together with Kv1.6 which over-rides this rapid inactivation via its NIP domain [16] were expressed in different positions with respect to each other. Two copies of Kv1.2 formed the other constituent of these hetero-tetramers. In one concatenated gene construct, Kv1.4 was separated from Kv1.6 with a single copy of Kv1.2, in another case, Kv1.6 was placed immediately adjacent to Kv1.4, followed by two copies of Kv1.2, the third tetramer had two copies of Kv1.2 between Kv1.4 and Kv1.6, giving three tetramers with identical subunit composition but different ordering of their subunits [Figure 1A].

All tetramer construction employed an inter-subunit linker derived from the *Xenopus* β-globin gene shown previously to be suitable [25]. Initial PCR of cDNA encoding Kv1.2, 1.6 or 1.4, yielded single bands on electrophoresis with the expected sizes of 1.5 and 2.0 kbp, respectively. Flanking inter-subunit linkers and paired restriction sites, allowing cloning into the pIRES2-DsRed expression vector, were added to the amplified products as described for pIRES2-EGFP [20]. The resultant hetero-tetramers, Kv1.4-1.2-1.6-1.2, Kv1.4-1.6-1.2-1.2 and Kv1.4-1.2-1.2-1.6, were assembled into pIRES-DsRed with the Kv1.4 gene introduced at the start (position I) to conserve functionality of its NIB. Kv1.6, where present, was placed either adjacently (position II or position IV) or distally (position III) to the Kv1.4 sequence (Supplemental Material, Figure S1). All concatenated constructs (Kv1.4-1.2-1.6-1.2, Kv1.4-1.6-1.2-1.2, and Kv1.4-1.2-1.2-1.6), upon transfection into HEK-293 cells, followed by surface biotinylation analysis, yielded an expressed protein band on SDS-PAGE of Mr ~ 240 k when probed with antibodies specific to Kv1.2, 1.4 or 1.6 (Figure 1B).

Plasmalemmal targeting of intact concatenated K^+ channels in active form

While biotinylation provided biochemical evidence of presence of intact concatenated hetero-tetramer at the plasmalemma, immuno staining on transfected mammalian cells was performed to determine the extent of trafficking from the ER to the plasmalemma. Labelling of HEK-293 cells expressing either Kv1.4-1.2-1.6-1.2, Kv1.4-1.6-1.2-1.2 or Kv1.4-1.2-1.2-1.6 with mouse IgGs specific for Kv1.2 and Kv1.4, followed by confocal fluorescence microscopy, detected clear immuno staining on the cell surface (Figure 1C). Untransfected cells (Figure 1C, bottom left panel) and cells transfected with Kv1.4-1.2-1.6-1.2 and incubated with secondary antibody only (bottom right panel), showed no staining. Similar levels of labelling were observed for hetero-tetramers (Kv1.4-1.2-1.6-1.2 and Kv1.4-1.6-1.2-1.2) in which the wild-type Kv1.6 was substituted with a mutated Kv1.6 (data not shown).

Kv1.6 subunit prevents fast inactivation of K^+ currents only when positioned adjacent to Kv1.4 in heteromeric channel proteins

When subjected to a 10-sec depolarisation step to +10 mV or -20 mV, the expressed Kv1.4-1.2-1.6-1.2 channel displayed a rapidly inactivating A-type K^+ current (Figure 2A) which is surprising as this heteromer contains a NIP domain known to disallow N-type fast inactivation [16]. Such rapid decay suggests that distal positioning of the NIP-containing Kv1.6 relative to Kv1.4, in this heteromer, attenuates NIP functionality. In stark contrast, heteromers Kv1.4-1.6-1.2-1.2 and Kv1.4-1.2-1.2-1.6, yielded a slow-inactivating currents (Figure 2A), as expected, due to the dominant negative effect of the NIP domain in Kv1.6 [16]. Current traces from the three heteromeric channels were best fitted with a double exponential function, which revealed significant differences in inactivation rates (Figure 2B, Table 1). Accordingly, the K^+ current resulting from heteromers where Kv1.4 and 1.6 are placed adjacently (Kv1.4-1.6-1.2-1.2 and Kv1.4-1.2-1.2-1.6), showed slower τ_{1inact} and $\tau_{2\ inact}$ values than those of Kv1.4-1.2-1.6-1.2 at -20 and 10 mV potentials, respectively (Figure 2B, Table 1). The fast inactivating channel (Kv1.4-1.2-1.6-1.2) gave fairly constant τ_{1inact} and $\tau_{2\ inact}$ values at different potentials (Figure 2B, Table 1), while the slow-inactivating channel counterparts revealed variable τ_{1inact} (but not $\tau_{2\ inact}$) values. Among the two slow-inactivating channels, differences in $\tau_{1\ inact.}$ values at more positive potentials can be correlated with shifting the Kv1.6 subunit from the second to the fourth position, which might affect the NIP functionality. A steady-state inactivation protocol demonstrated the influence of NIP positioning in the concatamers on the voltage dependence of inactivation. The resultant data, fitted by a single Boltzmann function (Figure 2C) unveiled a difference in the midpoints for voltage-dependent inactivation. Hetero-tetramers where Kv1.6 and 1.4 subunits are in adjacent positions showed $V_{1/2}$ values of -28 mV for Kv1.4-1.6-1.2-1.2, and -29 mV for Kv1.4-1.2-1.2-1.6 compared with -54 mV for Kv1.4-1.2-1.6-1.2; steady-state inactivation parameters are listed in Table 1. This shift in $V_{1/2}$ of the latter channel towards a more hyperpolarized voltage correlates with N-type inactivation due to distal positioning of the NIP, contrasting with that for the adjacently-arranged hetero-tetramers. Also, membrane potentials more negative than -70 mV were required to remove inactivation from all heteromers tested (Figure 2C). The recovery from inactivation was studied with a step from -90 to 10 mV, using a variable interval-gapped pulse protocol (see Figure 3A). Analysis of the time dependence of recovery from inactivation (Figure 3B) revealed that

this is significantly faster for Kv1.4-1.6-1.2-1.2 and Kv1.4-1.2-1.2-1.6, than that observed for Kv1.4-1.2-1.6-1.2 (Figure 3B), as a result of the removal of Kv1.4 N-type inactivation by the adjacently-placed Kv1.6 NIP. Inactivation kinetic values are summarised in Table1.

Mutagenesis proved that attenuation of N-type inactivation by Kv1.6 is mediated by NIP

Having demonstrated modulation of the Kv1.4 NIB by Kv1.6 within concatenated hetero-tetramers of pre-determined ordering, it was necessary to ascertain if these observed effects are entirely attributable to the NIP domain. Mutagenesis of residues in Kv1.6 α subunit identified previously as crucial for NIP function [16], and replacing the wild-type with mutated subunit (E32/30/27A), yielded channels [Kv1.4-1.2-1.6(E32/30/27A)-1.2 and Kv1.4-1.6(E32/30/27A)-1.2-1.2)] which both decay rapidly (Figure 4A1). These inactivation time courses are similar to those observed with heteromers containing distally-arranged wild-type Kv1.6 (Figure 4A1; Table 1), confirming a complete loss of NIP function from Kv1.6 is possible either by mutation or distal positioning of the wild-type, both permitting fast-inactivation of the K^+ current. Both mutated channels showed similar values of inactivation at both τ_{1inact} and τ_{2inact} at the different potentials tested (Figure 4A3, Table 1). This is attributable to the fast inactivation mediated by Kv1.4 subunit in each heteromer where NIP function is attenuated. This compares well with values derived from the distally arranged heteromer (Kv1.4-1.2-1.6-1.2) comprising 'wild type' 1.6, confirming that NIP in this position has no discernible effect on the NIB moiety.

These results were confirmed by the observed restoration of voltage dependence for inactivation ($V_{1/2}$~50 mV, Table 1) and recovery from inactivation for either channel containing the mutated Kv1.6 subunit (Figure 4A2, B1,2) to values similar to that of Kv1.4-1.2-1.6-1.2 (Figure 2B2; Table 1). Such corroborative data highlight that only the NIP domain in Kv1.6 prevents fast-inactivation, and this function is dependent on its position relative to the Kv1.4 subunit.

DISCUSSION

Arrangements of Kv1α genes in constructs determine subunit positions in the expressed channels

A new cloning platform was employed that afforded expression of 4 α subunits as a single protein, with pre-determined subunit ordering relative to each other in the functional channels examined on the plasmalemma. Importantly, and in contrast to previous systems [26], the use of inter-subunit linkers appears to have ensured retention of the behaviour of intermediately positioned subunits as illustrated by retention of NIP function of Kv1.6. Three such pre-assembled hetero-oligomers are presented, all with identical α subunit composition, but in different arrangements, containing a single Kv1.4 and 1.6 subunit plus two copies of 1.2. This offered the advantage over previous studies [16] in allowing the effects of their positioning to be examined. Hetero-tetramers (Kv1.4-1.2-1.6-1.2, Kv1.4-1.6-1.2-1.2 and Kv1.4-1.2-1.2-1.6) elicited K^+ currents, with one, displaying significantly different inactivation properties to the other two. Such dissimilarity, together with the uniform nature of the currents produced by each

concatenated tetramer, established that the gene arrangements in the constructs dictate subunit ordering.

Subunit ordering reveals position-dependency of NIP function

This confirmed retention of subunit ordering and delivery of intact hetero-tetramers to the plasmalemma allowed the generation of channels exhibiting different types of inactivation by incorporating just one copy of Kv1.4 and 1.6, rather than two as examined previously [16]. Moreover, the concatenation of these subunits along with Kv1.2, combinations reported to co-exist in brain [15], permitted elucidation of the importance of their ordering. The NIP in Kv1.6 proved functional only if placed immediately next to (position II or IV) its target Kv1.4 (position I) in the formed channel, yielding a slow-inactivating K^+ current. Positioning Kv1.6 distal to Kv1.4 (position III) led to N-type fast inactivation, presumably, because NIP is not optimally positioned to appropriately antagonize the activity of NIB. Furthermore, the same fast inactivation kinetics were observed with NIP-mutated forms of these channels, confirming that only the NIP domain is responsible for counter-acting the function of NIB. Such position-dependency of NIP activity could accord with a previous suggestion [16] that this domain does not act by occupying the acceptor site for NIB, instead, interacting directly with the latter.

NIP, NIB and inactivation outcomes

It was of interest to consider the observed inactivation profiles in relation to occupancy (or not) by NIB of its receptor site on the S6 segment of the channel because this mechanism is the basis of N-type inactivation [4,5,24,25]. A reported inability of homo-tetrameric Kv1.6 [13,16] to produce a fast-inactivating K^+ current implies that NIP is unable to bind to the inner pore, at least in a blocking fashion. The system validated herein for creating heteromers which exhibit fast (distal channels) or slow (adjacent channels) inactivation provides scope for evaluating their distinct biophysical properties. In this way, the adjacent concatamers were found to recover faster from inactivation than the rapidly-inactivating distally-arranged protein; this accords with the rate of recovery from inactivation being enhanced by a slow inactivation (C-type) mechanism [27]. It is noteworthy that the observed rates of fast inactivation for the mutated adjacent- and distal-concatemers are similar, suggesting that positioning of a non-functional NIP domain does not impact on their fast inactivation. Moreover, the fast inactivation behavior of Kv1.4-1.6(E32/30/27A)-1.2-1.2 channels showed clearly that NIP and NIB domains are directly interacting, upon depolarisation, mainly by electrostatic interaction before the NIB reaches its receptor, by an as-yet undefined mechanism. One can speculate that conformational changes, initiated by the activation process, would be sensed by both charged motifs of the NIP and NIB domains facilitating their interaction. Positioning of both domains away from each other would prevent such interaction, as seen with both Kv1.4-1.2-1.6(E32/30/27A)-1.2 and Kv1.4-1.2-1.6-1.2 channels.

In situ hybridization and immuno-histochemical localization studies suggested that Kv1.2, Kv1.4 and Kv1.6 proteins may co-exist on the membranes of several types of central neurons in mammals [15,18,28,29,30]. In rat brain membranes, hetero-multimeric Kv1 channels, with direct association of Kv1.4 and Kv1.6 subunits, were observed using subunit-specific antibodies in immuno-affinity experiments [15,16]. Collectively, these

findings suggest that the gating contributions of Kv1.4 subunits can be modified by differential positioning of the NIP domain of Kv1.6 subunit in neuronal Kv1 channels.

In co-expression studies, recombinant Kvβ1 has been shown to confer rapid inactivation, via its distinct NIB domain, on all tested members of Kv1 α subunits except Kv1.6, suggesting that Kvβ1 subunit could, also, be an important modulator of K^+ channel complexes [6,7]. In fact, Kv1.2, 1.4, and 1.6 α subunits in rat brain membranes can be co-immunoprecipitated with Kvβ1 [31]. These findings indicate that, in neurons, the gating of Kv1 heteromers can be modified by NIB/NIP domain(s) and/or auxiliary β1 subunits. In either case, the Kv1.6 subunit position in the heteromeric Kv1 channel could play a key role, in tuning the inactivation process and, thus, shaping the firing pattern of the neuron.

One is tempted to speculate on the functional relevance of NIP action in diseased states. Seizure activity in an animal model has been linked to the spatio-temporal changes in the expression of the Kv1 subfamily within the hippocampus [18], where the levels of delayed rectifier Kv1 channels (including Kv1.2 and Kv1.6) are reduced with minor changes in Kv1.4. This curious alteration might be a physiological response to seizure events in which Kv1.4 inactivation by NIP gets diminished, thereby, dampening unwanted depolarisations during attacks. Extensive investigations would have to be performed to assess the *in vivo* functional implications of NIP and its placement within native hetero-tetramers.

It is clear from the data presented herein that: (a) concatenation of Kv1 subunits results in the predicted assembly of functional channels at the plasmalemma; (b) subunit ordering crucially influences channel properties; (c) composition alone is not sufficient for predicting the characteristics of native channels and (d) NIP-NIB interaction(s) occur at a site distinct from that of NIB binding site in the inner portion of the ion pore.

ACKNOWLEDGMENT

The authors thank Prof. Olaf Pongs for generously providing Kv1 constructs, Dr. Jiafu Wang for assistance in evaluating the Kv1 constructs and concatenation strategy, Dr. Jon Sack for valuable comments on the manuscript and Dr. Saak Ovespian for help with the confocal microscopy and comments on the manuscript.

FUNDING

This work was funded by a Principle Investigator grant and a Research Professorship award by Science Foundation Ireland to J.O.D. and a PRTLI 4 grant from the Irish Higher Education Authority for the Neuroscience sections of 'Target-driven therapeutics and theranostics'.

REFERENCES

1. Scott, V.E., Muniz, Z. M., Sewing, S., Lichtinghagen, R., Parcej, D. N., Pongs, O. and Dolly, J. O. (1994) **Antibodies specific for distinct Kv subunits unveil a heterooligomeric basis for subtypes of alpha-dendrotoxin-sensitive K+ channels in bovine brain.** Biochemistry **33**,1617–1623
2. Yao, X, Segal, A. S., Welling, P., Zhang, X., McNicholas, C. M., Engel, D., Boulpaep, E. L., and Desir, G. V. (1995) Primary structure and functional expression of a cGMP-gated potassium channel. Proc. Natl. Acad. Sci. **92**, 11711-11715
3. Stuhmer, W., Ruppersberg, J. P., Schroter, K. H., Sakmann, B., Stocker, M., Giese,K. P., Perschke, A., Baumann, A., and Pongs, O. (1989) Molecular basis of functional diversity of voltage-gated potassium channels in mammalian brain. EMBO J. **8**, 3235–3244.
4. Hoshi, T., Zagotta, W. N., and Aldrich, R. W. (1990) Biophysical and molecular mechanisms of Shaker potassium channel inactivation. Science **250**, 533-538
5. Zagotta, W. N., Hoshi, T., and Aldrich, R. W. (1990) Restoration of inactivation in mutants of Shaker potassium channels by a peptide derived from ShB. Science **250**, 568-571
6. Rettig, J., Heinemann, S. H., Wunder, F., Lorra, C., Parcej, D. N., Dolly, J. O., and Pongs, O. (1994) Inactivation properties of voltage-gated K+ channels altered by presence of beta-subunit. Nature **369**, 289-294
7. Heinemann, S. H., Rettig, J., Graack, H. R., and Pongs, O. (1996) Functional characterization of Kv channel beta-subunits from rat brain. J. Physiol. **493**, 625-633
8. Morales, M. J., Wee, J. O., Wang, S., Strauss, H. C., and Rasmusson, R. L. (1996) The N-terminal domain of a K+ channel beta subunit increases the rate of C-type inactivation from the cytoplasmic side of the channel. Proc. Natl. Acad. Sci. U S A **93**, 15119-15123
9. Choi, K. L., Aldrich, R. W., and Yellen, G. (1991) Tetraethylammonium blockade distinguishes two inactivation mechanisms in voltage-activated K+ channels. Proc. Natl. Acad. Sci. U S A **88**(12), 5092-5095
10. Kiss, L., and Korn, S. J. (1998) Modulation of C-type inactivation by K+ at the potassium channel selectivity filter. Biophys. J. **74**(4), 1840-1849
11. Liu, Y., Jurman, M. E., and Yellen, G. (1996) Dynamic rearrangement of the outer mouth of a K+ channel during gating. Neuron **16**(4), 859-8
12. Yellen, G., Sodickson, D., Chen, T. Y., and Jurman, M. E. (1994) An engineered cysteine in the external mouth of a K+ channel allows inactivation to be modulated by metal binding. Biophys. J. **66**, 1068-1075
13. Stuhmer, W., Ruppersberg, J. P., Schroter, K. H., Sakmann, B., Stocker, M., Giese, K. P., Perschke, A., Baumann, A., and Pongs, O. (1989) Molecular basis of functional diversity of voltage-gated potassium channels in mammalian brain. EMBO J. **8**(11), 3235-3244
14. Sheng, M., Liao, Y. J., Jan, Y. N., and Jan, L. Y. (1993) Presynaptic A-current based on heteromultimeric K+ channels detected in vivo. Nature **365**, 72-7515. Shamotienko, O. G., Parcej, D. N., and Dolly, J. O. (1997) Subunit combinations defined for K+ channel Kv1 subtypes in synaptic membranes from bovine brain. Biochemistry **36**(27), 8195-8201
16. Roeper, J., Sewing, S., Zhang, Y., Sommer, T., Wanner, S. G., and Pongs, O.

(1998) NIP domain prevents N-type inactivation in voltage-gated potassium channels. Nature **391**, 390-393
17. Pfaffinger, P. J., and DeRubeis, D. (1995) Shaker K+ channel T1 domain self-tetramerizes to a stable structure. J. Biol. Chem. **270**(48), 28595-28600
18. Lee, S. M., Kim, J. E., Sohn, J. H., Choi, H. C., Lee, J. S., Kim, S. H., Kim, M. J., Choi, I. G., and Kang, T. C. (2009) Down-regulation of delayed rectifier K+ channels in the hippocampus of seizure sensitive gerbils. Brain Res. Bull. **80**(6), 433-442
19. Edwards, L., Nashmi, R., Jones, O., Backx, P., Ackerley, C., Becker, L., and Fehlings, M. G. (2002) Upregulation of Kv 1.4 protein and gene expression after chronic spinal cord injury. J. Comp. Neurol. **443**(2), 154-167
20. Al-Sabi, A., Shamotienko, O., Ni Dorghartaigh, S., Muniyappa, N., LeBerre, M., Sack, J. T., and Dolly, J. O. (2010) Arrangement of Kv1 alpha subunits dictates sensitivity to tetraethylammonium. J. Gen. Physiol. **136**: 273-82
21. Sokolov, M. V., Shamotienko, O., Dhochartaigh, S. N., Sack, J. T., and Dolly, J. O. (2007) Neuropharmacology Concatemers of brain Kv1 channel alpha subunits that give similar K+ currents yield pharmacologically distinguishable heteromers. **53**, 272-282
22. Manganes, L. N., and Trimmer, J. S. (2000) Subunit composition determines Kv1 potassium channel surface expression. J. Biol. Chem. **275**, 29685-93.
23. Ruppersberg, J. P., Stocker, M., Pongs, O., Heinemann, S. H., Frank, R., and Koenen, M. (1991) Regulation of fast inactivation of cloned mammalian IK(A) channels by cysteine oxidation. Nature **352**(6337), 711-714
24. Tseng-Crank, J., Yao, J. A., Berman, M. F., and Tseng, G. N. (1993) Functional role of the NH2-terminal cytoplasmic domain of a mammalian A-type K channel. J. Gen. Physiol. **102**(6), 1057-1083
25. Akhtar, S., Shamotienko, O., Papakosta, M., Ali, F., and Dolly, J. O. (2002) Characteristics of brain Kv1 channels tailored to mimic native counterparts by tandem linkage of alpha subunits: implications for K+ channelopathies. J Biol. Chem. **277**(19), 16376-16382
26. Gagnon, D. G., and Bezanilla, F. (2009) A single charged voltage sensor is capable of gating the Shaker K+ channel. J. Gen. Physiol. **133**(5), 467-483
27. Rasmusson, R. L., Morales, M. J., Castellino, R. C., Zhang, Y., Xampbell, D. L., and Strauss H.C. (1995) C-type inactivation controls recovery in a fast inactivating cardiac K+ channel (Kv1.4) expressed in Xenopus oocytes. J. Physiol. **489**, 709-721
28. Veh, R. W., Lichtinghagen, R., Sewing, S., Wunder, F., Grumbach, I. M., and Pongs, O.(1995) Immunohistochemical localization of five members of the Kv1 channel subunits: contrasting subcellular locations and neuron-specific co-localizations in rat brain. Eur. J. Neurosci. **7**(11), 2189-205.
29. Chung, Y. H., Joo, K. M., Nam, R. H., Kim, Y. S., Lee, W. B., and Cha, C. I. (2005) Immunohistochemical study on the distribution of the voltage-gated potassium channels in the gerbil cerebellum. Neurosci. Lett. **374**(1), 58-62.
30. Kim, D. S., Kim, J. E., Kwak, S. E., Won, M. H., and Kang, T. C. (2007) Seizure activity affects neuroglial Kv1 channel immunoreactivities in the gerbil hippocampus. Brain. Res. **1151**, 172-187
31 Rhodes, K. J., Strassle, B. W., Monaghan, M. M., Bekele-Arcuri, Z., Matos, M.F., and Trimmer, J. S. (1997) Association and colocalization of the Kvbeta1 and Kvbeta2 beta-subunits with Kv1 alpha-subunits in mammalian brain K+ channel complexes.

J. Neurosci. **17**:8246-58

FIGURE LEGENDS

Figure 1. Concatenation of Kv1.X genes, expression and trafficking of complete hetero-tetrameric Kv1 channels to the plasmalemma of mammalian cells. (**A**) Schematic of concatenated constructs of Kv1 genes (symbolised), in a single ORF within pIRES2-DsRed plasmid with requisite linkers, and predicted subunit arrangements in the expressed proteins. NIB and NIP refer to the Kv1.4 N-terminal inactivation ball and its prevention domain in Kv1.6, respectively. (**B**) Transiently transfected HEK-293 cells expressing Kv1.4-1.6-1.2-1.2, (lanes 1, 4 and 7), Kv1.4-1.2-1.6-1.2 (2, 5 and 8), or Kv1.4-1.2-1.2-1.6 (3, 6 and 9). Intact cells were biotinylated, detergent solubilised, precipitated with streptavidin-agarose beads and analysed by Western blotting using antibodies specific for either Kv1.2 (lanes 1-3), Kv1.4 (4-6) or Kv1.6 (7-9); k, denotes a molecular weight marker (kDa). (**C**) Confocal fluorescence micrographs showing surface expression of hetero-tetrameric channels in transfected HEK-293 cells, after incubation with a monoclonal antibody reactive to either Kv1.2 or Kv1.4. The labelling was visualised by using anti-species IgGs coupled to Alexa Fluor 488. Control cells transfected with Kv1.4-1.6-1.2-1.2 (bottom left panel) and non-transfected cells (bottom right) were stained only with secondary antibody). Scale bar denotes 5 μm.

Figure 2. Inactivation kinetics of K^+ currents are strongly dependent on the position of Kv1.6 relative to Kv1.4 in the concatamers. (**A**) Representative current traces, in response to a two-pulse steady-state inactivation protocol, for each depicted channel. (**B**) The bar diagrams summarise the τ_1 and τ_2 rates of inactivation for the representative channels at different potentials. See Table 1 for the significant difference (*) between representative values ($P < 0.05$, Mann-Whitney *U*-test). (**C**) The steady-state inactivation relationship, taken from normalised peak currents triggered by pre-pulse potentials and fitted with a single Boltzmann function (see Experimental Procedures). This plot shows a significant ($P < 0.05$, Mann-Whitney *U*-test) voltage shift for Kv1.4-1.6-1.2-1.2 (○, broken line) and Kv1.4-1.2-1.2-1.6 (▲, broken line) to more positive potentials compared to Kv1.4-1.2-1.6-1.2 channels (●), as a result of Kv1.6 NIP functionality. See Table 1 for values.

Figure 3. Recovery from inactivation is faster when Kv1.6 is adjacent to Kv1.4 in the concatamers (**A**) Recovery from inactivation measured for Kv1.4-1.2-1.6-1.2 Kv1.4-1.6-1.2-1.2 and Kv1.4-1.2-1.2-1.6, using variable interval-gapped pulse protocol (inset, bottom panel). (**B**) The resultant curves, fitted with a single exponential function show a significantly faster ($P < 0.05$, Mann-Whitney *U*-test) recovery from inactivation for Kv1.4-1.6-1.2-1.2 (○, broken line) and Kv1.4-1.2-1.2-1.6 (▲, broken line) than observed for the Kv1.4-1.2-1.6-1.2 channel (●). This is due to the removal of Kv1.4 N-type inactivation by the Kv1.6 NIP domain. Inactivation constants are shown in Table 1. Curves display the average values from at least 4 cells. Some error bars fall within the data symbols; the points in the broken lines are super-imposed; dotted lines indicate zero current.

Figure 4. Position-dependent functioning of Kv1.6 is NIP mediated: replacement of Kv1.6 with a mutant form abolished NIP activity, thereby, restoring rapid inactivation. (**A1**) Representative current traces for channels with mutated Kv1.6 (E32/30/27/A)

incorporated (Kv1.4-1.6-1.2-1.2 and Kv1.4-1.2-1.6-1.2) and expressed in HEK-293 cells. (**A2**) Steady-state inactivation relationships obtained for these channels, fitted by a Boltzmann function [broken line for Kv1.4-1.6-1.2-1.2 (□) and straight line for Kv1.4-1.2-1.6-1.2 (■)], revealed near-identical profiles. Dotted lines indicate zero current. (**A3**) The bar diagrams summarise the τ_1 and τ_2 rates of inactivation of both channels taken at different potentials. (**B1**) Typical currents showing recovery from inactivation of each hetero-tetramer fitted to a single exponential function. (**B2**) When plotted, the average data for each channel, from at least 4 cells gave super-imposable curves; some error bars fall within the data points.

Biochemical Journal Immediate Publication. Published on 25 Feb 2011 as manuscript BJ20102169

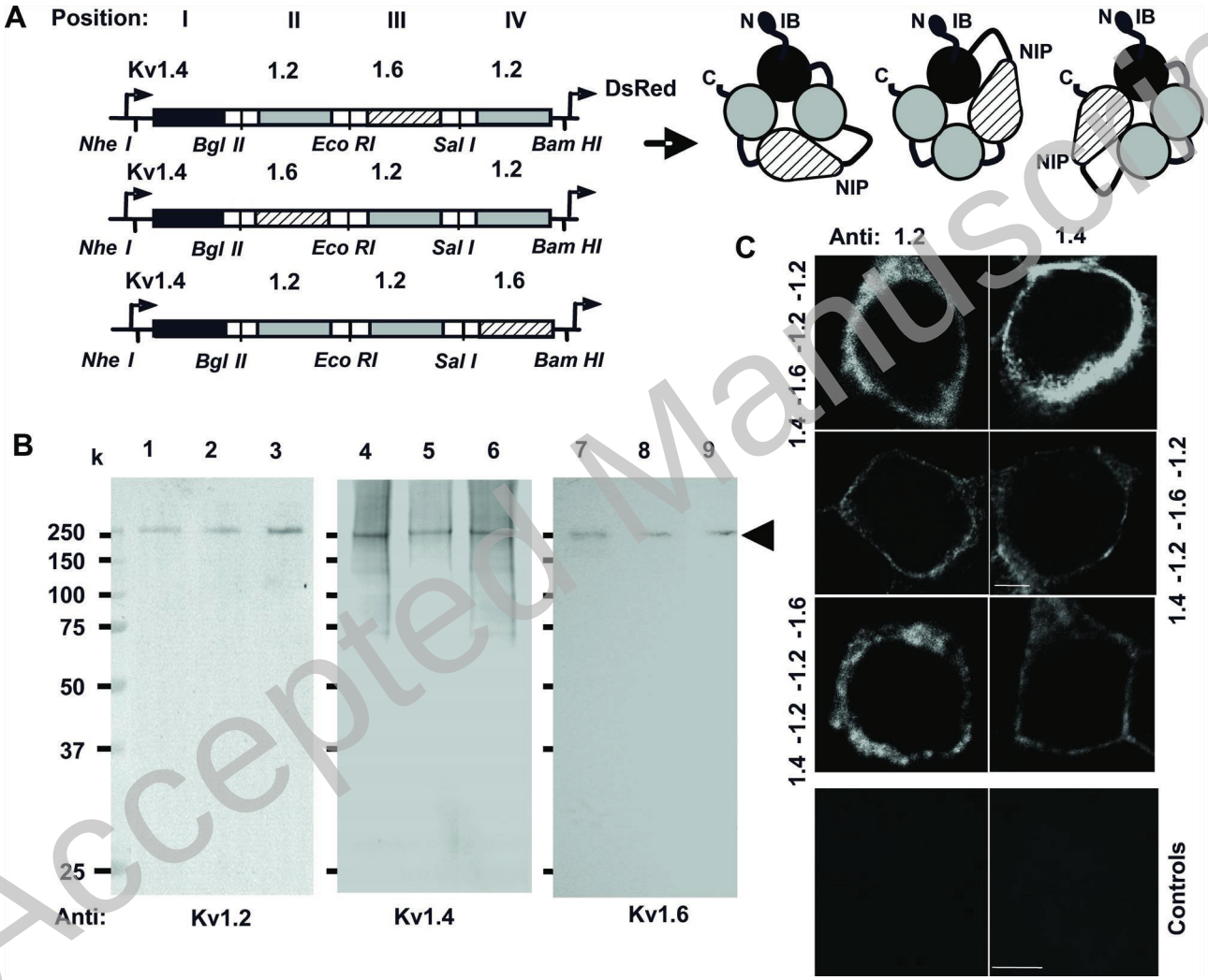

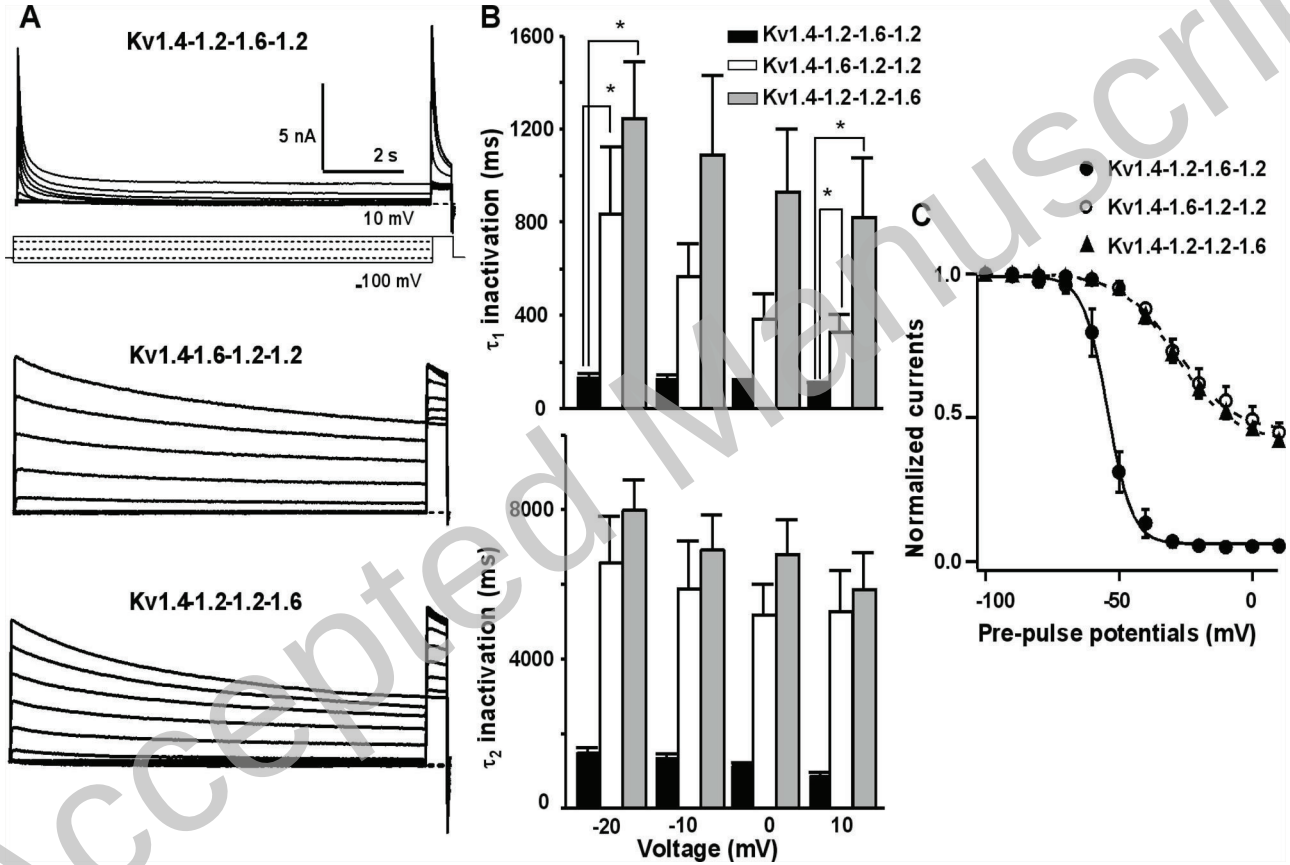

Biochemical Journal Immediate Publication. Published on 25 Feb 2011 as manuscript BJ20102169

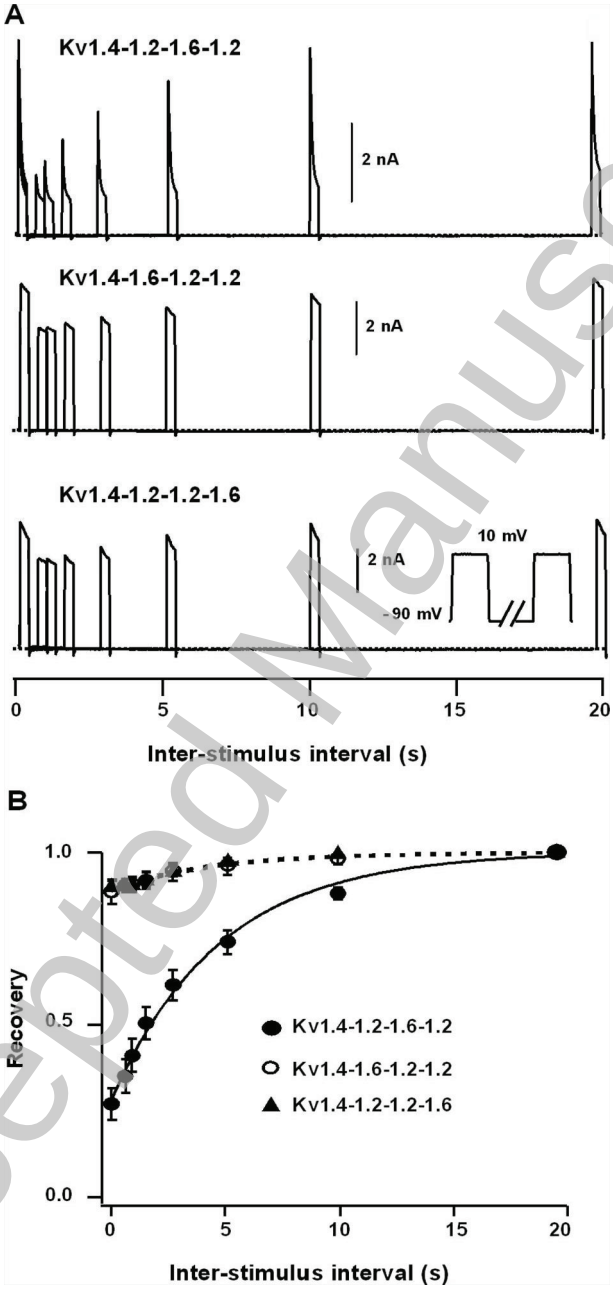

Biochemical Journal Immediate Publication. Published on 25 Feb 2011 as manuscript BJ20102169

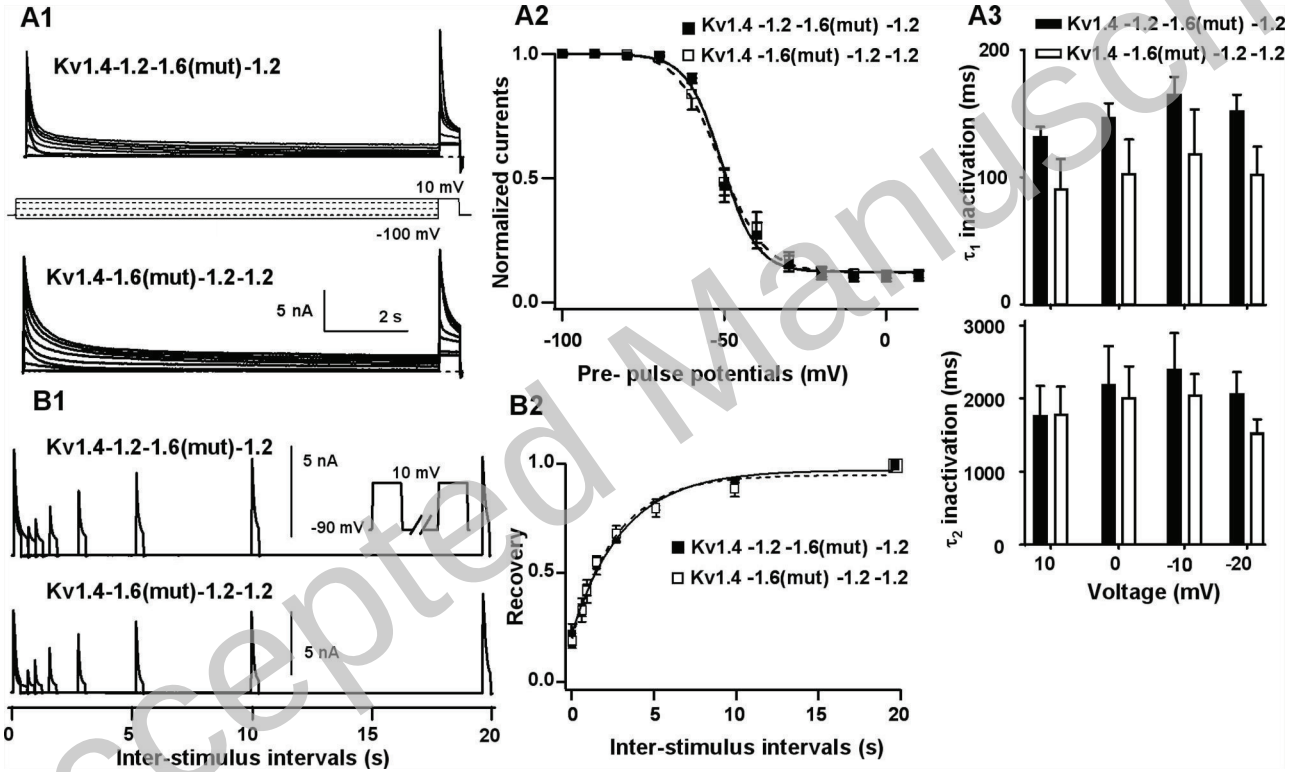

TABLE 1 Summary of inactivation parameters for Kv1.4-containing heteromers expressed in HEK-293 cells

Channels	**Inactivation time constants**				**Steady state inactivation**		**Recovery from inactivation**
	$\tau_{1inact.}$ at 10 mV (ms)	$\tau_{2inact.}$ at 10 mV (ms)	$\tau_{1inact.}$ at -20 mV (ms)	$\tau_{2inact.}$ at -20 mV (ms)	$V_{1/2}$ (mV)	Slope (*k*)	τ at -90 mV (s)
Kv1.4-1.6-1.2-1.2	*330 ± 80 (8)	*5290 ± 1090	*840 ± 290 (8)	*6590 ± 1220	*-28 ± 1 (5)	10 ± 1	*4.8 ± 0.02 (6)
Kv1.4-1.2-1.2-1.6	*820 ± 260 (4)	*5860 ± 1000	*1240 ± 240 (4)	*7970 ± 830	*-29 ± 1 (4)	10 ± 1	*4.2 ± 0.03 (4)
Kv1.4-1.6(mut)-1.2-1.2	90 ± 24 (4)	1780 ± 380	102 ± 22 (4)	1520 ± 190	-51 ± 1 (8)	7 ± 1	3.2 ± 0.03 (5)
Kv1.4-1.2-1.6-1.2	*100 ± 16 (5)	*850 ± 120	*130 ± 20 (5)	*1470 ± 175	*-54 ± 2 (5)	5 ± 1	*3.6 ± 0.02 (7)
Kv1.4-1.2-1.6(mut)-1.2	130 ± 8 (5)	1750 ± 420	150 ± 13 (5)	2060 ± 300	-51 ± 1 (9)	5 ± 1	2.7 ± 0.1 (4)

* Values are significant, $P < 0.05$ (Mann-Whitney *U*-test). Data recorded are presented as means ± S.E.M., n-values are in brackets.